9.4 Microstructural Development During Slow Cooling

We are now in a position to follow closely the **microstructural development** in various binary systems. In all cases, we shall assume the common situation of cooling a given composition from a single-phase melt. Microstructure is developed in the process of solidification. We consider only the case of *slow* cooling; that is, equilibrium is essentially maintained at all points along the cooling path. The effect of more rapid temperature changes is the subject of Chapter 10, which deals with time-dependent microstructures developed during heat treatment.

Let us return to the simplest of binary diagrams, the case of complete solubility in both the liquid and solid phases. Figure 9.32 shows the gradual solidification of the 50% A–50% B composition treated previously (Figures 9.6, 9.8, and 9.30). The lever rule (Figure 9.31) is applied at three different temperatures in the two-phase (L + SS) region. It is important to appreciate that the appearance of the microstructures in Figure 9.32 corresponds directly with the relative position of the overall system composition along the tie line. At higher temperatures (e.g., T_1), the overall composition is near the liquid-phase boundary, and the microstructure is predominantly liquid. At lower temperatures (e.g., T_3), the overall composition is near the solid-phase boundary, and the microstructure is predominantly solid. Of course, the compositions of the liquid and solid phases change continuously during cooling through the two-phase region. At any temperature, however, the relative amounts of each phase are such that the overall composition is 50% A and 50% B, which is a direct manifestation of the lever rule as defined by the mass balance of Equation 9.8.

The understanding of microstructural development in the binary eutectic is greatly aided by the lever rule. The case for the eutectic composition itself is straightforward and was illustrated previously (Figures 9.12 and 9.15). Figure 9.33 repeats those cases in slightly greater detail. An additional comment is that the composition of each solid-solution phase (α and β) and their relative amounts

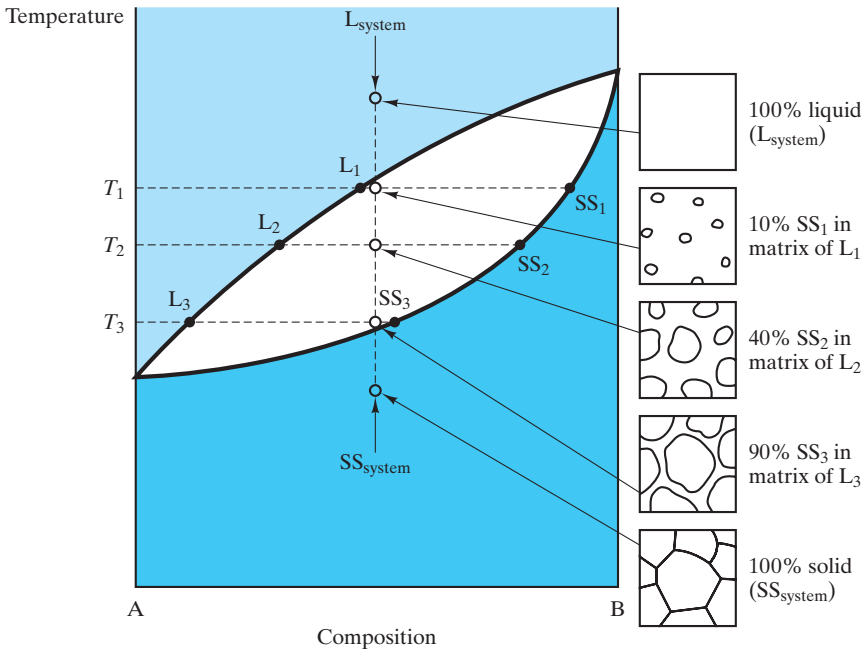

FIGURE 9.32 *Microstructural development during the slow cooling of a* 50% A–50% B *composition in a phase diagram with complete solid solution. At each temperature, the amounts of the phases in the microstructure correspond to a lever-rule calculation. The microstructure at T_2 corresponds to the calculation in Figure 9.30.*

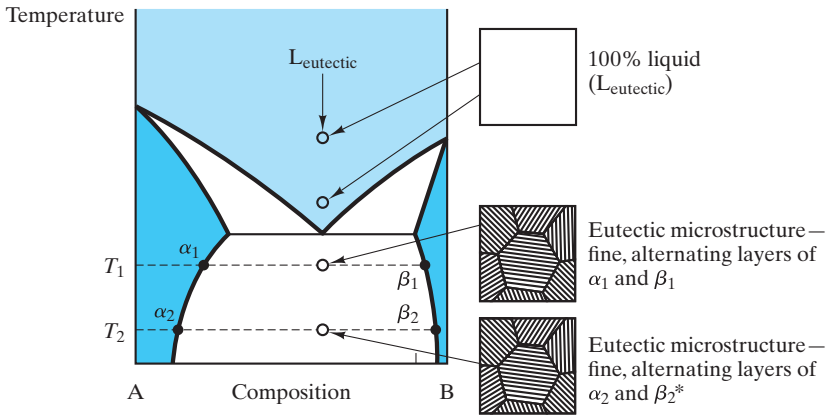

*The only differences between this structure and the T_1 microstructure are the phase compositions and the relative amounts of each phase. For example, the amount of β will be proportional to

$$\frac{x_{eutectic} - x_\alpha}{x_\beta - x_\alpha}.$$

FIGURE 9.33 *Microstructural development during the slow cooling of a eutectic composition.*

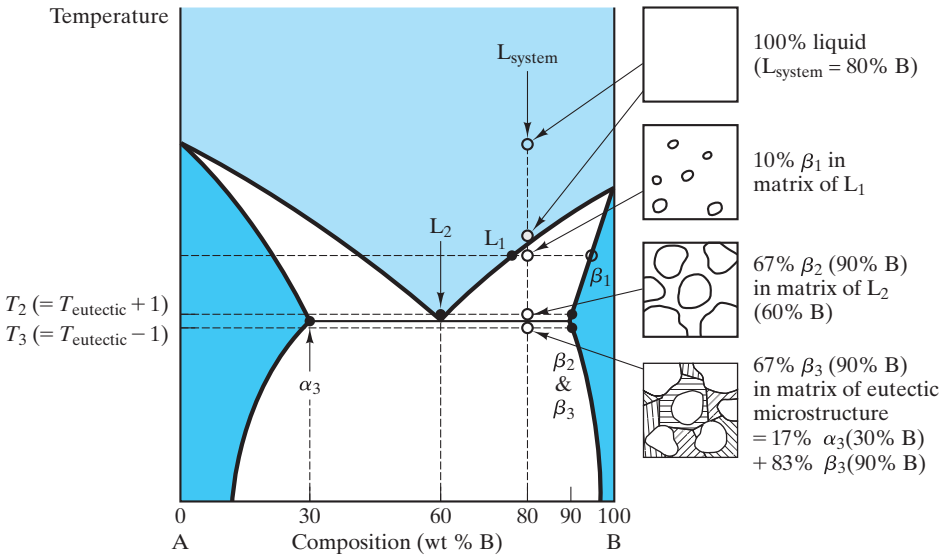

FIGURE 9.34 *Microstructural development during the slow cooling of a hypereutectic composition.*

will change slightly with temperature below the eutectic temperature. The microstructural effect (corresponding to this compositional adjustment due to solid-state diffusion) is generally minor.

Microstructural development for a noneutectic composition is more complex. Figure 9.34 illustrates the microstructural development for a **hypereutectic composition** (composition greater than that of the eutectic). The gradual growth of β crystals above the eutectic temperature is comparable to the process found in Figure 9.32 for the complete solid-solution diagram. The one difference is that, in Figure 9.34, the crystallite growth stops at the eutectic temperature with only 67% of the microstructure solidified. Final solidification occurs when the remaining liquid (with the eutectic composition) transforms suddenly to the eutectic microstructure upon cooling through the eutectic temperature. In a sense, the 33% of the microstructure that is liquid just above the eutectic temperature undergoes the eutectic reaction illustrated in Figure 9.33. A lever-rule calculation just below the eutectic temperature (T_3 in Figure 9.34) indicates correctly that the microstructure is 17% α_3 and 83% β_3. However, following the entire cooling path has indicated that the β phase is present in two forms. The large grains produced during the slow cooling through the two-phase (L + β) region are termed **proeutectic** β; that is, they appear "before the eutectic." The finer β in the lamellar eutectic is appropriately termed *eutectic* β.

Figure 9.35 shows a similar situation that develops for a **hypoeutectic composition** (composition less than that of the eutectic). This case is analogous to that for the hypereutectic composition. In Figure 9.35, we see the development of large grains of proeutectic α along with the eutectic microstructure of α and β layers. Two other types of microstructural development are illustrated in Figure 9.36. For an overall composition of 10% B, the situation

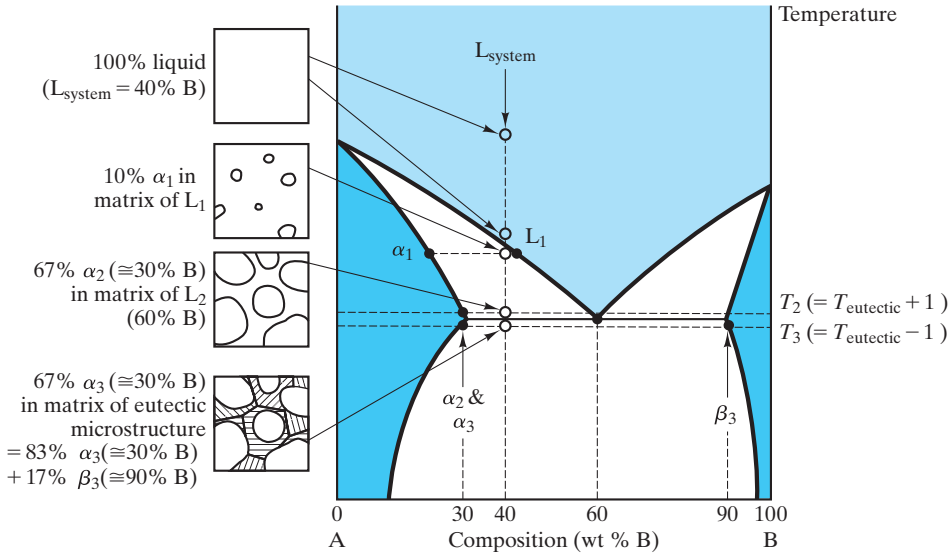

FIGURE 9.35 *Microstructural development during the slow cooling of a hypoeutectic composition.*

is quite similar to that for the complete solid-solution binary in Figure 9.32. The solidification leads to a single-phase solid solution that remains stable upon cooling to low temperatures. The 20% B composition behaves in a similar fashion except that, upon cooling, the α phase becomes saturated with B atoms. Further cooling leads to precipitation of a small amount of β phase. In Figure 9.36(b), this precipitation is shown occurring along grain boundaries. In some systems, the second phase precipitates within grains. For a given

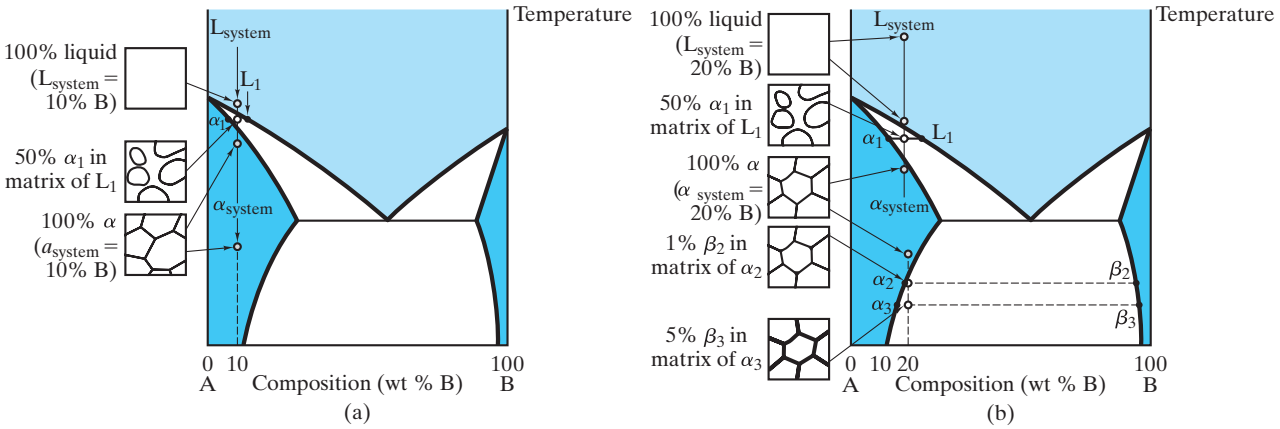

FIGURE 9.36 *Microstructural development for two compositions that avoid the eutectic reaction.*

system, the morphology of the second phase can be a sensitive function of the rate of cooling. In Section 10.4, we shall encounter such a case for the Al–Cu system, in which precipitation hardening is an important example of heat treatment.

With the variety of cases encountered in this section, we are now in a position to treat any composition in any of the binary systems presented in this chapter, including the general diagrams represented by Figure 9.25(b).

The cooling path for a **white cast iron** (see also Chapter 11) is shown in Figure 9.37. The schematic microstructure can be compared with a micrograph in Figure 11.1(a). The eutectoid reaction to produce pearlite is shown in Figure 9.38. This composition (0.77 wt % C) is close to that for a 1080 plain-carbon steel (see Table 11.1). Many phase diagrams for the Fe–Fe_3C system give the eutectoid composition rounded off to 0.8 wt % C. As a practical matter, any composition near 0.77 wt % C will give a microstructure

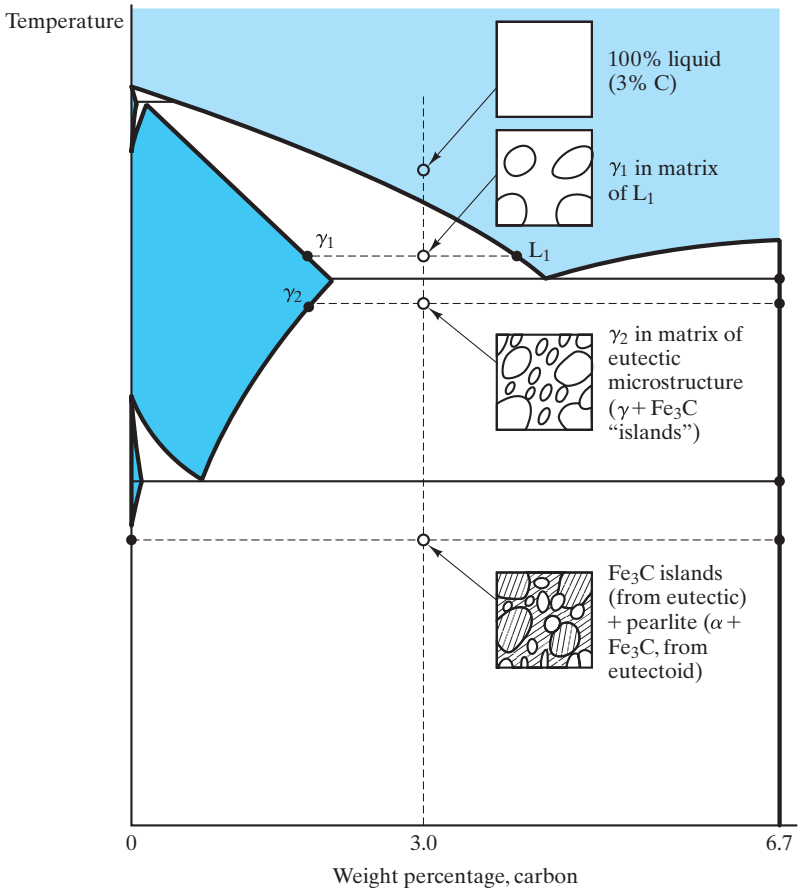

FIGURE 9.37 *Microstructural development for white cast iron (of composition* 3.0 *wt % C) shown with the aid of the* Fe−Fe_3C *phase diagram. The resulting (low-temperature) sketch can be compared with a micrograph in Figure 11.1(a).*

EXAMPLE 9.6

Figure 9.34 shows the microstructural development for an 80 wt% B alloy. Consider instead 1 kg of a 70 wt % B alloy.

(a) Calculate the amount of β phase at T_3.

(b) Calculate what weight fraction of this β phase at T_3 is proeutectic.

SOLUTION

(a) Using Equation 9.10 gives us

$$m_{\beta,T_3} = \frac{x - x_\alpha}{x_\beta - x_\alpha}(1\text{ kg}) = \frac{70 - 30}{90 - 30}(1\text{ kg})$$

$$= 0.667\text{ kg} = 667\text{ g}.$$

that is predominantly eutectoid. The actual pearlite microstructure is shown in the micrograph of Figure 9.2.

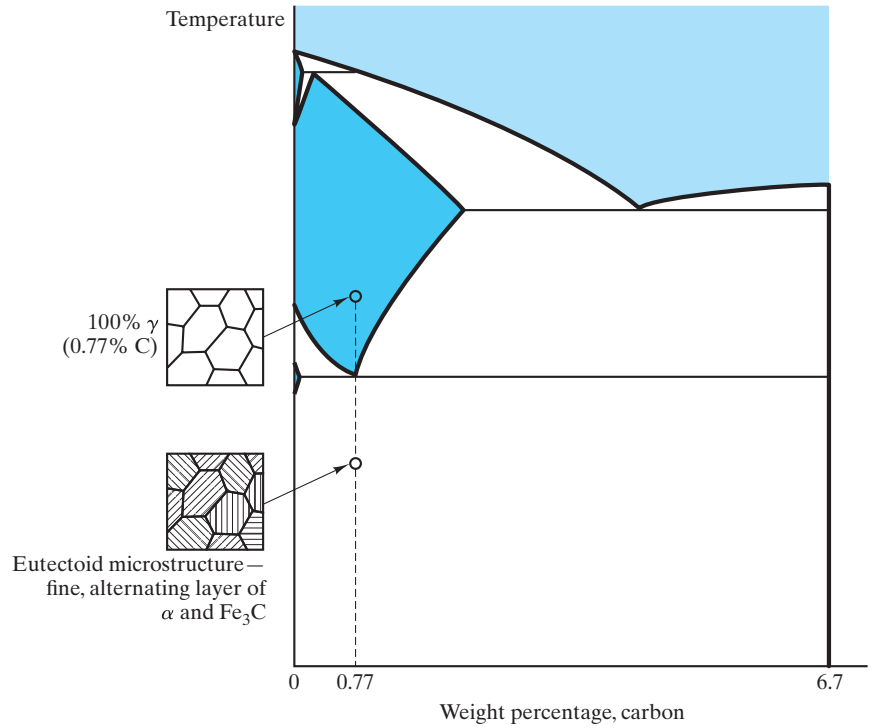

FIGURE 9.38 *Microstructural development for eutectoid steel (of composition 0.77 wt % C). The resulting (low-temperature) sketch can be compared with the micrograph in Figure 9.2.*